

A MODEL FOR KINKING IN FIBER COMPOSITES— I. FIBER BREAKAGE VIA MICRO-BUCKLING

PAUL S. STEIF

Department of Mechanical Engineering, Carnegie-Mellon University, Pittsburgh,
PA 15213, U.S.A.

(Received 7 November 1988; in revised form 9 March 1989)

Abstract—Kink band formation in uniaxially compressed fiber composites is studied theoretically. A model is proposed which involves the bowing of a bundle of slightly misaligned fibers (via micro-buckling) until fiber fracture, followed by a finite deformation which brings the fibers into the kinked configuration. These two critical steps in the process are treated separately in this two-part paper. In Part I, the critical strain at which the fibers can break is calculated; in Part II the critical strain at which a fully formed kink band can exist is calculated. It is found that the critical strain to form the fiber breaks is comparable to observed compressive failure strains and is, in general, greater than the strain at which a fully formed kink band can exist. This appears to imply that the formation of the fiber breaks is the limiting step in kinking. The theory is consistent with the seminal features of kinking, including: the fiber breaks at the kink band boundary, the relatively small width of the kinks, and the typical orientation relation between the kinked fibers and the kink band boundary. Computations based on the model reveal the dependence of kinking on pertinent material variables.

INTRODUCTION AND BACKGROUND

There are a variety of reasons for fiber-reinforced composites to be weak when compressed parallel to the fibers. In some cases, for example in polymeric-based fibers, the fibers themselves are relatively weak in compression. In other cases, there is insufficient constraint to prevent longitudinal splitting, in which a crack runs parallel to the fibers in the compression direction. Of course, structural buckling can be a problem for slender members. For advanced composites that are intended to withstand substantial compressive loads, however, the typical mode of failure is fiber kinking. In a unidirectional composite, kinking generally involves bands of material that have undergone intense shearing, and in which the fibers are re-oriented—up to 60° or more—from their original direction. Since this failure mechanism can be a limiting one for some composite systems, it is of interest to increase the fundamental understanding of this failure mechanism with the hope of designing materials with greater resistance to kinking. In this two-part sequence of papers, a theoretical model for the formation of kink bands is proposed. Efforts by a number of investigators have been directed towards studying compressive failure; not surprisingly, the proposed theory is, in part, a reorganization of previous models. Much of the theory, however, involves substantially new approaches.

Early on, compressive failures of this type were viewed as coinciding with fiber micro-buckling. Responding to the suggestion of Dow and Gruntfest (1960) that individual fibers buckle under longitudinal compression, Rosen (1965) put forth the first—and still most quoted—model for compressive failure. He idealized a buckling fiber as a beam on an elastic foundation, the foundation simulating the effect of the matrix and the surrounding fibers on the fiber in question. The buckling load, which he took to signal compressive failure, was found to be on the order of the elastic shear modulus of the matrix. Unfortunately, this is significantly in excess of observed compressive strengths, and no refinement (e.g. Sadowsky *et al.*, 1967; Herrmann *et al.*, 1967; Chung and Testa, 1969; Greszczuk, 1975; Steif, 1987; Waas *et al.*, 1989) of Rosen's (1965) elastic micro-buckling analysis has significantly lowered his prediction of compressive strength.

Rosen himself immediately recognized that the strength was overestimated by his theory, and he suggested that plasticity in the matrix reduces the shearing resistance and could, therefore, account for the discrepancy. Given the strains at which compressive failure

occurs, however, no reduction in the shearing resistance can be expected if one continues to insist that the fibers begin as perfectly straight. However, the *combined* effect of fiber misalignment and yielding of the matrix was suggested by Argon (1972) to reduce predictions of compressive strength to more acceptable values. Elaborating upon this idea somewhat, Budiansky (1983) has argued that the resistance of fibers to micro-buckling in a plastic matrix is highly sensitive to fiber misalignment. Both Budiansky (1983) and Hahn (1987) have attempted to make a connection between micro-buckling (with imperfections and matrix plasticity) and the formation of kink bands. An alternative explanation for observed compressive strengths involving the failure of the fiber-matrix interface under shear—which can occur in the presence of misaligned fibers if the interface is weak—was suggested by Piggott (1981). Steif (1988) has recently considered the effect of a weak interface (which for most models of a micro-buckling fiber is essentially equivalent to matrix plasticity), and he has explored micro-buckling by studying the linear amplification of an initial imperfection. In most of the early studies, the wavelength of the micro-buckling fiber (which, we argue below, determines the kink width) was tacitly assumed to be equal to the specimen length. By contrast, the theoretical approaches of Budiansky (1983) and Hahn (1988) predict kink band widths which are roughly on the order of observed widths.

These efforts, in particular the micro-buckling analyses, have been less than adequate in that they have not come to grips with the seminal features of kinking in fibrous composites. The detailed observations of kinking in three-dimensional carbon-carbon composites by Evans and Adler (1978), as well as the observations of compressively loaded unidirectional carbon-epoxy composites under confining pressure by Weaver and Williams (1975), point out the following: (i) kinking involves fiber fracture at the kink boundaries; (ii) kink widths are much smaller than the specimen length; and (iii) there exist relatively consistent relations between the kink angle and the kink band boundary.

Based on a careful consideration of observations of kinking, we offer the following sketch of the process whereby a kink band forms under longitudinal compression. In the fabrication of real composites, the fibers will not be perfectly aligned; most likely a bundle of fibers within the composite will be misaligned, as depicted in Fig. 1a. Under a compressive load parallel to the fibers, the fibers bend accentuating this misalignment (Fig. 1b). Under sufficient compression, the fibers break and the kink forms as shown in Fig. 1c. Within this framework, the width of the kink band is determined by the wavelength of the imperfection which causes micro-buckling. It should be pointed out that although our analysis is predicated upon the kink initiating from a misaligned bundle, kink bands often initiate from free edges or from cutouts. The elements of the model as currently formulated would presumably have their counterparts in cases of other initiating imperfections.

We believe it is appropriate to view the whole process of kinking as having two essential steps. First, the fibers break at the necessary points due to micro-buckling of the fibers.

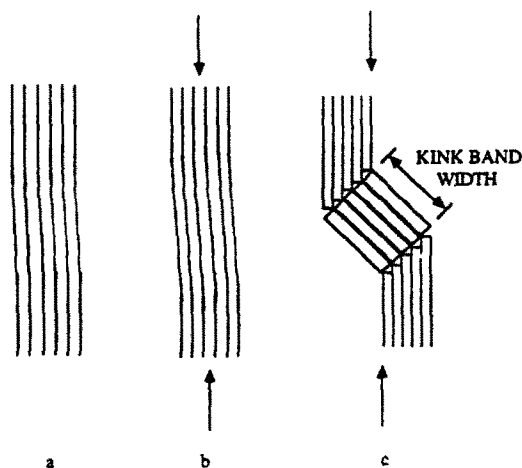


Fig. 1. Schematic of the sequence of events in the process of kinking.

Secondly, the material between the breaks deforms as a kink. In connection with the micro-buckling step, it should be pointed out that previous approaches to micro-buckling share the drawback of focusing on the *initiation* of buckling. Yet the fiber needs to do more than just buckle, it needs to bend sufficiently far to cause fracture of the fibers. This idea of tensile fracture of the fibers in bending, which was originally suggested by Berg and Salama (1973), may be an important element in a proper theory of compressive failure. To date, this notion of achieving a critical tensile strain in bending has not been combined with an analysis of the buckling of fibers under compression. Also, there has been relatively little modeling of the process of kink band development (with the exception of Evans and Adler, 1978; Budiansky, 1983; Hahn, 1987); in particular, a computation of the applied load to induce kinking has not been carried out.

A model for compressive failure by kinking is reported here as a two-part paper, each part focusing on a crucial aspect of the kinking process. Part I deals with the initiation of the fiber breaks via micro-buckling. Part II is concerned with the formation of a complete kink band. These aspects will be treated separately, except that the computations for the kink band will *presume* the existence of the necessary fiber breaks. The critical strains for each of these processes—fiber breaks via micro-buckling and kinking with pre-existing breaks—will be calculated and compared. The process which has the higher critical strain will be the limiting step in that it will determine the load at which kinking actually occurs.

The calculation of the remote compressive strain at which initially unstraight fibers fail in tension due to bending is based on an extension of a previous model (Steif, 1988). A fiber initially having a slight waviness is permitted to undergo *finite* deflections (but infinitesimal strains), under the action of a longitudinal compressive load and resistance provided by the matrix, surrounding fibers and interface. Allowing finite deflections is essential to an accurate implementation of the critical bending strain criterion, though properly accounting for them requires a nonlinear analysis. Nevertheless, it is relatively straightforward to solve the relevant elastica problem numerically. Results of the numerical solutions will be compared with experiments; in addition, they allow the dependence of the fiber breaking strain on a range of pertinent material variables to be explored.

ANALYSIS

Obviously, an analysis of the simultaneous deformations of many fibers in a composite subjected to compression is prohibitive. The task is simplified somewhat if one is able to argue that the deformations of different fibers form some pattern. For example, Rosen (1965), in his early work, proposed two distinct micro-buckling modes: a shear mode (fibers deforming in-phase with one another) and an extensional mode (fibers deforming out-of-phase with one another). While it is unlikely that an entire specimen goes into any single mode, micrographs of kink band formation (and our summarizing Fig. 1) suggest that the bundle in which the kink initiates does, in fact, deform in the shear mode. (It is difficult to imagine an out-of-phase mode in a real three-dimensional composite.) Once some deformation pattern is postulated, one can consider the compressive loading of a single representative fiber which is constrained by the surrounding material, the constraint being determined by the overall deformation pattern. Because the shear mode appears not to cause a change in fiber separations, we follow Rosen and take the surrounding material to resist the fiber deformation only by applying shear stresses to the fiber. Note that these shear stresses arise *within* the misaligned bundle due to the deformation of the bundle in the shear mode. On the other hand, the rest of the composite (outside the misaligned bundle) may resist the shear deformation of the bundle with normal forces; the potential significance of this resistance will be taken up below after presenting the results.

A free-body diagram of an element of the representative fiber in the plane of the shear mode is shown in Fig. 2. The quantity τ represents the average shear stress in the plane that arises due to the deformation; as indicated, there are equal and opposite shear stresses acting on the fiber. If the fiber is assumed to be circular with radius a , then, by integrating around the fiber circumference, the shear stresses communicate a couple to the fiber which is equal to $4a^2\tau$. The applied longitudinal compressive force is denoted by P , M is the



Fig. 2. Free-body diagram of an element of a micro-buckling fiber.

bending moment in the fiber, V is the transverse shear force, and θ is the orientation of the fiber segment relative to the compression axis. For the analysis of bending, we assume the fiber is inextensible; therefore, the deformation of the fiber is described completely by giving the rotation θ as a function of position along the fiber.

From a simple moment balance, the following equation of equilibrium is obtained

$$\frac{dM}{ds} + P \sin \theta - 4a^2 \tau = 0 \quad (1)$$

where s is arclength along the segment. Since there is no net lateral force (the shearing resistance is a pure couple), the transverse shear force V is zero everywhere, and the longitudinal force P is constant along the length. Note that P and V are defined with respect to fixed axes.

At this point, the constitutive laws must be incorporated. We assume the strains in the fiber are infinitesimal, even though the deflection is arbitrarily large. Treating the fiber as an elastica, we take the moment at each point to be proportional to the local curvature; hence,

$$M = E_f I \frac{d\theta}{ds} \quad (2)$$

where E_f is the fiber modulus and I is the polar moment of inertia, which equals $\pi a^4/2$ for a circular fiber.

It is the constitutive law relating the shear stress τ to the fiber rotation which is perhaps the most speculative aspect of micro-buckling models. The problem is that the shear stress and strain really vary from point to point around the fiber. Here, we adopt the simple approach originating with Rosen (1965): fibers rotating in phase with one another cause some *average* shear strain in the matrix. For infinitesimal rotations, the shear strain is clearly proportional to the rotation. Using some simplifying assumptions, Rosen (1965) gives expressions for the average shear stress and shear strain which are dependent on the fiber volume fraction and the matrix shear modulus. We believe that no modeling could ever establish an accurate relation between the average shear stress τ and the fiber rotation for a real three-dimensional composite. As an alternative, we will simply take the shear stress τ —for small rotations—to be equal to

$$\tau = G_L \theta$$

where G_L is interpreted as being *roughly* equal to the longitudinal elastic shear modulus of the composite. Since it is the matrix which is directly in contact with the fibers, it may be that the elastic shear modulus of the matrix is more appropriate to use. The sensitivity to the value of this modulus will be explored in the results section.

It will also be assumed that once the rotation becomes substantial, the shear stress communicated to the fiber reaches some limiting maximum value τ_c . For convenience, we incorporate this assumed response by taking the shear stress to depend on the rotation in the following manner

$$\tau = \tau_c \tanh \frac{G_L \theta}{\tau_c}. \quad (3)$$

This relation is linear for small θ ($\tau = G_L \theta$), and monotonically approaches a maximum value τ_c as θ becomes large compared with τ_c/G_L . Our purpose in adopting this relation is to have a smooth, analytically tractable relation which simulates an elastic–perfectly plastic response. Since we eventually obtain solutions numerically, any relation between shear stress and fiber rotation could be incorporated into the computations. One sensible alternative, a truly elastic–perfectly plastic relation (with a jump in slope) was also considered; it was found to lead to very similar results. In this connection we contend that the errors associated with the present model of compressive failure will be greater than any differences occasioned by slight variations in the shear stress–fiber rotation relation. In addition, it is unlikely that one could experimentally determine more than two parameters, one characteristic of the elastic response (G_L) and one characteristic of the limiting strength (τ_c). Given the accuracy of using G_L above, it would appear acceptable to identify τ_c with the longitudinal shear strength of the composite, with the matrix shear strength, or with the interfacial shear strength, whichever is appropriate.

Finally, the imperfection which takes the form of an initial waviness of the fiber bundle (and of the representative fiber, in particular) is incorporated in a mathematically tractable way by assuming an initial sinusoidal variation in the fiber slope $\theta = \theta_0$, given by:

$$\theta_0 = e \cos \frac{\pi s}{L} \quad (4)$$

where the imperfection has an amplitude e and a wavelength $2L$, a parameter which will prove to be crucial to the ultimate results. This initial waviness exists with no stress; hence, the shear stress τ is actually related to the angle $\theta - \theta_0$, as is the moment M . Since the θ appearing in $P \sin \theta$ is geometric (and not constitutive), it remains unchanged.

By symmetry, one need only consider a quarter wavelength. The governing differential equation can be derived by combining eqns (1)–(4) to arrive at

$$\theta'' + k \sin \theta - \alpha T_f \tanh \frac{\theta - \theta_0}{T_f} = -e \cos x \quad (5)$$

where the domain is $0 < x < \pi/2$, ()' denotes differentiation with respect to the independent variable x , and the dimensionless variables are defined by:

$$x = \frac{\pi s}{L}, \quad k = \frac{PL^2}{\pi^2 E_f I}, \quad \alpha = \frac{4a^2 G_L L^2}{\pi^2 E_f I}, \quad T_f = \frac{\tau_c}{G_L}.$$

The quantity x is the dimensionless arclength, k is the normalized load, α can be viewed as representing the stresses associated with elastically shearing the matrix relative to those associated with bending the fiber, and T_f is roughly the rotation at which the shearing resistance starts to go plastic. The boundary conditions are zero moment at $x = 0$, and zero slope at $x = \pi/2$; hence,

$$\theta'(0) = 0, \quad \theta(\pi/2) = 0. \quad (6a,b)$$

A simple shooting method was used to solve eqn (5) subject to the boundary conditions (6), given some fixed value of k . Beginning with $\theta(\pi/2) = 0$, a value of $\theta'(0)$ was guessed and the differential equation was integrated using a fourth-order Runge–Kutta method to $x = 0$. If $\theta'(0)$ was not zero, the guess for $\theta'(\pi/2)$ was adjusted appropriately.

The quantity of interest will be the maximum tensile strain in the bending fiber; when this equals the tensile fracture strain of the fiber ε_f , fiber fracture can occur. The maximum tensile strain in the fiber is the sum of two terms: the bending strain which is arrived at by

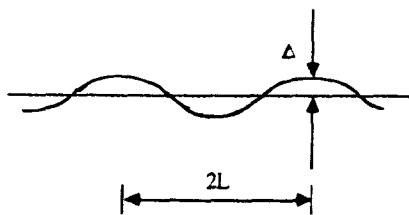


Fig. 3. Definition of parameters describing imperfectly aligned fiber bundle.

solving (5), and the compressive strain ϵ_{comp} associated with the longitudinal compressive load P . Since the compressive failure strain of the composite is on the order of ϵ_f , the latter contribution must be included. (Note, however, that the bending contribution is calculated on the basis of an inextensible elastica.) Since the longitudinal force P acts parallel to the fiber at the point where the bending is maximum, one can express the second contribution in terms of k as

$$\epsilon_{\text{comp}} = -\frac{\pi^2}{2} k \frac{a^2}{L^2}. \quad (7)$$

The overall compressive strain at which the fibers fracture is referred to as the fiber-breaking strain.

Before presenting numerical results, we consider an evaluation of the governing parameters from readily available composite materials data. Values for E_f , a , G_L , and τ_c are often quoted; they allow one to compute $\alpha' \equiv \alpha(a/L)^2$ and $T_f = \tau_c/G_L$. Remaining are the imperfection amplitude e and the imperfection wavelength $2L$, the latter clearly having an upper limit of the specimen length. The imperfection amplitude is certainly not a material property; in fact, there are many imperfections in a given composite, and different imperfections have different amplitudes. Nevertheless, for an imperfection of a given wavelength, the amplitude e should be reflective of the *average* degree of fiber misalignment in the composite.

To capture a reasonable dependence of e upon L we replace e and introduce the parameter Δ . We considered Δ to be fixed, and we took e and L to be related according to

$$e = \frac{\Delta}{L}.$$

Recall that e is the maximum initial *angle* of rotation; as indicated in Fig. 3, Δ has dimensions of length. Hence, for a fixed Δ , the imperfection amplitude is less for longer wavelength imperfections. This was chosen so as to be in accord with the sense that a relatively long wavelength imperfection with too large an amplitude e would correspond to an inordinately large matrix-rich zone next to the misaligned bundle. It seemed that Δ , or Δ/a , is a better measure of the inherent fiber misalignment of the composite as a whole; to consider various degrees of fiber misalignment, one can consider various values of Δ/a .

RESULTS

First, we consider some qualitative features of solutions to the governing eqn (5). For relatively short wavelengths, and other parameters having typical values, the load increases monotonically with the maximum bending strain $\theta'(\pi/2)$. More interesting, however, is the

character of the solutions for moderate to long wavelengths, as shown in Fig. 4. The load reaches a local maximum, decreases to a local minimum, after which the load increases indefinitely with $\theta'(\pi/2)$. When the load depends on the bending strain in this manner, the condition for fiber fracture at $x = \pi/2$ was generally found to be reached at a bending strain which exceeds that corresponding to the load maximum (see Fig. 4). If such is the case, then the correct failure load may be that corresponding to the local load minimum. In practice, however, the difference is rather small; results for the fiber-breaking strain presented below were based on the load which gave precisely the failure strain at $x = \pi/2$.

Consider now a comparison between the predictions of the fiber-breaking strain based on the present theory and the predictions of two approximate approaches that one might be inclined to use. It was pointed out by Argon (1972) that misaligned fibers and plasticity in the matrix reduce the micro-buckling load; using our variables, the compressive strength he suggested was

$$\sigma_c = \frac{\tau_c}{e} \tag{8}$$

One means of arriving at this result was put forth by Steif (1988), who carried out an analysis of the problem considered here, except with linearized kinematics ($\sin \theta \approx \theta$) and the elastic-perfectly plastic relation

$$\tau = \begin{cases} G_L \theta & \theta < \tau_c/G_L \\ \tau_c & \theta > \tau_c/G_L \end{cases} \tag{9a}$$

$$\tag{9b}$$

instead of (3). A version of this analysis, now in terms of the slope θ instead of the deflection as was done by Steif (1988), is given in the Appendix.

As the analysis indicates, the matrix responds elastically along the entire fiber if $k < T_f(1+\alpha)/(T_f+e)$, at which point matrix plasticity initiates at $x = 0$; the plasticity spreads to $x = \pi/2$ as the load increases. This load to initiate plasticity is equivalent to Argon's compressive strength (8) if $T_f \ll e$ and $\alpha \gg 1$. It may also be seen from the analysis given in the Appendix that the resulting angle θ can be infinite if plasticity has initiated before $k = 1$, which is the buckling load when there is no matrix restraint (buckling of an Euler column). Clearly, this linear analysis is invalid at this level of loading. The conclusion arrived at by Steif (1988) was that compressive failure coincided with the initiation of matrix plasticity, after which there would be catastrophic buckling.

A second approximate approach to this problem, which gives results that are qualitatively consistent with the behavior illustrated in Fig. 4, is to perform an initial post-buckling analysis of (5) (see Budiansky, 1974). Considering, first, a perfectly aligned fiber, one finds that it has a symmetric bifurcation point at $k = \alpha + 1$, after which the load decreases rapidly,

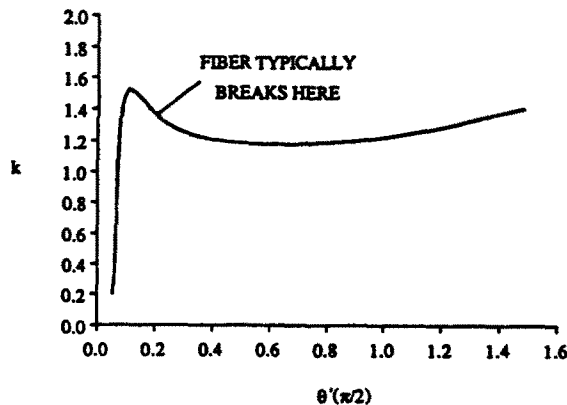


Fig. 4. Load versus end rotation of micro-buckling fiber showing nonlinear response.

particularly if T_f is small compared with 1. Hence, with a small degree of misalignment e , there is a maximum load, k_{\max} , which is given by

$$k_{\max} = (\alpha + 1) \left\{ 1 - 3 \left(\frac{e}{2} \right)^{2/3} \left[\frac{\frac{\alpha}{T_f^2} - \frac{1}{2}(\alpha + 1)}{4(\alpha + 1)} \right]^{1/3} \right\}. \quad (10)$$

Thus, the initial post-buckling analysis predicts the local maximum in the load.

To illustrate the potential error of equating compressive failure with either the load to induce matrix plasticity based on the linearized analysis or the maximum load based on the initial post-buckling analysis, these estimates are compared with accurate numerical results in Table 1. (The parameter values are $\alpha' = 0.0123$, $T_f = 0.025$, $\Delta/a = 1.0$, $\epsilon_f = 0.048$, which are appropriate to the glass fiber bundle embedded in Epon 828 considered below.) Note that $L/a = 18$ corresponds to an initial misalignment of roughly 3° . The maximum load based on the initial post-buckling analysis (labeled "Perturbation Solution" in Table 1) is in error because the imperfection is not sufficiently small to justify the underlying perturbation assumption; it would be correct if the imperfection were extremely small. On the other hand, the load to induce plasticity over-estimates the fiber-breaking strain for long wavelengths and underestimates it for short wavelengths—hardly a reliable means of estimating compressive failure.

Specific predictions of the model are now compared with data presented by Hahn and Sohi (1986) on the compressive failure of fiber bundles embedded in epoxy. Performing this comparison suggests realistic ranges of parameters; it also gives some indication of the reasonableness of the theory. The experiments of Hahn and Sohi (1986) involved bundles of four different types of fibers each embedded in two different epoxies. Their method of embedding a bundle in a block of epoxy allows the final failure state of the bundle to be preserved, because the surrounding epoxy does not fail at the failure strain of the bundle. This permitted them to assess the lengths of the kinked segments, as well as the failure strain. The lengths of the kinked segments would presumably be related to the kink band width in a real composite. They found that the lengths of the kinked segments varied from one combination to another, but were roughly within a range of 5 to 13 times the fiber diameter.

Hahn and Sohi (1986) provided values for the fiber moduli and failure strains, and the epoxy moduli and ultimate strengths. Thus, the quantities α' , T_f , and ϵ_f may be calculated. (It is difficult to say what the longitudinal shear properties of the bundle itself is, since the fiber fraction is not well defined; hence, α' and T_f were defined in terms of the shear properties of the matrix.) Initially, a fiber offset of one fiber radius ($\Delta = a$) was assumed, and the fiber-breaking strain ϵ_b was computed for a range of lengths L/a . Recalling that the wavelength is $2L$, one can see that the length of a kinked segment (spanning from one fiber break to the next, from a peak to the next trough) would be L . This, together with the experimentally observed segment lengths, dictated the range that was chosen for L/a . The fiber-breaking strains computed by the theory developed above, as well as the observed bundle failure strains, are presented in Table 2.

According to the theory just presented, the fiber-breaking strain depends strongly on the wavelength of the imperfection. In fact, if a constant value of e were to be assumed, instead of Δ , the decrease in ϵ_b with L/a would be even sharper. Remarkably, however, the wavelengths at which the theoretical fiber-breaking strains agree with the observed bundle

Table 1. Comparison of numerical solution for k at failure with approximate methods

L/a	8.0	10.0	12.0	14.0	18.0	22.0	30.0	40.0	50.0
Numerical solution	0.767	0.863	0.952	1.035	1.186	1.323	1.574	1.879	2.21
Linearized solution	0.298	0.446	0.640	0.884	1.547	2.467	5.173	10.34	17.639
Perturbation solution	-2.945	-3.255	-3.569	-3.871	-4.394	-4.755	-4.841	-3.535	-0.476

Table 2. Theoretical fiber breaking strains ϵ_b for various embedded bundle combinations

Fiber	Matrix	Theoretical failure strain L/a					Experimental
		8.0	10.0	12.0	14.0	18.0	
E-Glass	Epon 828	0.059	0.043	0.033	0.026	0.018	0.039
E-Glass	Epon 815	0.056	0.040	0.030	0.024	0.016	0.021
Graphite (T700)	Epon 828	0.047	0.033	0.026	0.020	0.014	0.024
Graphite (T700)	Epon 815	0.045	0.032	0.024	0.019	0.013	0.020
Graphite (T300)	Epon 828	0.044	0.032	0.025	0.020	0.014	0.023
Graphite (T300)	Epon 815	0.043	0.030	0.023	0.018	0.013	0.019

failure strains are roughly within the range of observed kink band widths. This suggests that the breaking of the fibers is the critical step in the formation of the kink band. Further evidence of this is presented in Part II, in which the actual formation of the kink band—with fiber breaks already present—is considered.

The dependence of the fiber-breaking strain on the parameters Δ , ϵ_f , α' and T_f , is shown in Figs 5 through 8, respectively. The dependence on Δ is significant, particularly for smaller wavelengths. However, the sensitivity may be somewhat less than more approximate models have suggested. According to Argon's failure prediction (8), which can also be arrived at by a linear analysis of the present problem, the compressive strength is inversely proportional to the imperfection. On the other hand, if one considers the variation with Δ , for constant L/a , the sensitivity is seen to be less, sometimes substantially less.

As shown in Fig. 6, the dependence of the fiber-breaking strain on the fiber failure strain ϵ_f is very slight, particularly for long wavelengths. Perhaps this is not surprising: the process of bowing the fiber is highly nonlinear. For a long fiber, once the load is high

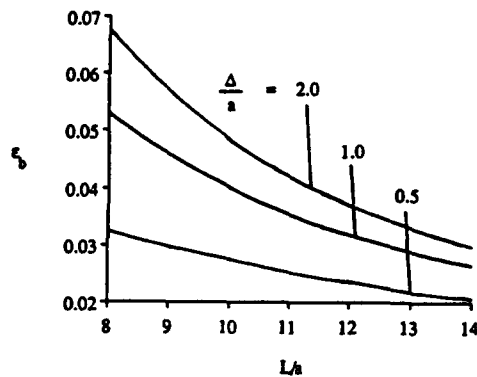


Fig. 5. Fiber breaking strain for various imperfection magnitudes Δ/a ($\alpha' = 0.0132$, $T_f = 0.025$, $\epsilon_f = 0.0183$).

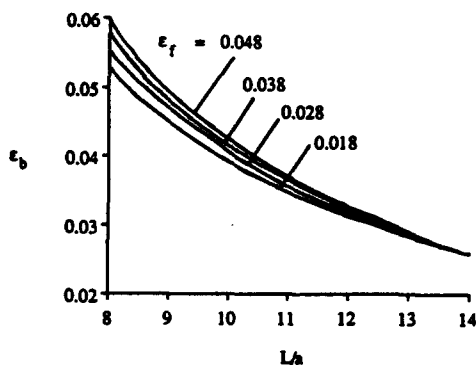


Fig. 6. Fiber breaking strain for various fiber ductilities ϵ_f ($\alpha' = 0.0123$, $T_f = 0.025$, $\Delta/a = 1.0$).

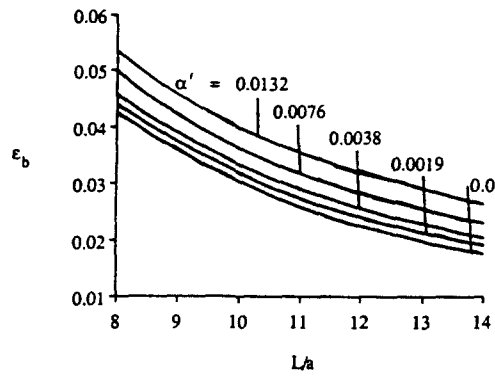


Fig. 7. Fiber breaking strain for various values of normalized matrix shear modulus α' ($\Delta/a = 1.0$, $T_f = 0.025$, $\varepsilon_f = 0.0183$).

enough for the critical strain to be reached, much higher bending strains can be reached without much increase in load. This is supported by Fig. 4, which indicates the maximum bending strain as a function of the load k . Clearly, a significant range of bending strains can be achieved with virtually no change in the load. It should be also noted that Hahn and Sohi (1986) found that all the fiber bundles (except the P75 graphite fibers, which suffered shear failure themselves) failed essentially at a strain of 2%, except for the glass fibers in Epon 828. Hence, even if the Berg and Salama (1973) tensile strain criterion has to be satisfied, it is relatively insensitive to the actual value of the critical strain.

The dependence on α' is also rather modest. In fact, to see how small its effect is, consider the lowest curve in Fig. 7, which corresponds to $\alpha = 0$: this is tantamount to no matrix support. This is quite at odds with Rosen's (1965) prediction that the micro-buckling load scales with the matrix shear modulus. One can explain this by recalling that the classical micro-buckling result (see, for example, Greszczuk, 1982) has an additional term that depends on $E_f(a/L)^2$. This bending contribution is usually neglected because the wavelength was generally assumed to be on the order of the specimen length. When the wavelength is on the order of the observed kink widths, however, the bending contribution becomes dominant. It should be noted, therefore, that letting the initial shearing resistance in eqn (2) be equal to the longitudinal shear modulus G_L is acceptable, in that small variations in this parameter would have little effect.

The dependence on T_f is shown in Fig. 8 for a range in T_f . It was found by Piggot and Harris (1980) that the ratio of an epoxy's strength to its modulus is generally 1/50 to 1/40: thus, the range of values chosen for T_f . Lower values of T_f are possible, however, and can be detrimental. They would arise if the shear stress transmitted to the fibers were limited not by the matrix shear strength but by the interfacial strength, which can be rather low. The post-buckling analysis performed earlier gives some indication of the potential

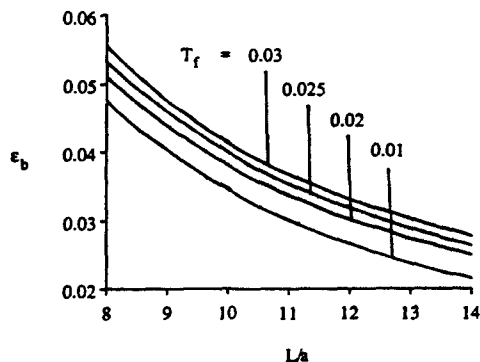


Fig. 8. Fiber breaking strain for various values of normalized matrix shear strength T_f ($\alpha' = 0.0132$, $\Delta/a = 1.0$, $\varepsilon_f = 0.0183$).

decrease in the compressive strength which is occasioned by low values of T_f . However, the effect is not nearly as strong as one might expect, because of the dominance of the bending contribution, as mentioned above.

The model formulated here appears to be the first model of kinking or micro-buckling that connects the observed failure strain with the observed kink band width L . Nevertheless, the question remains: what determines the kink band width? For instance, why doesn't the composite fail at a lower strain with a wider kink band? One possible explanation is now offered.

Recall that *within* the misaligned bundle which ultimately forms the kink, the fibers are taken to deform together in the shear mode. It is this shear mode which gives a diminishing failure strain with increasing wavelength. (Rosen (1965) found this too, though his micro-buckling loads were much higher than those found here.) However, the misaligned bundle itself is surrounded by presumably well aligned material which acts to resist the deformation of the misaligned bundle. This constraint on the bundle as a whole is the same constraint that acts on a single fiber which is part of Rosen's extension mode, with the straight fiber adjacent to the misaligned bundle constituting the symmetry plane (see Fig. 9).

Rosen's (1965) early calculation of the so-called extensional mode is still appropriate, except that it is the misaligned bundle that is buckling not an individual fiber. This mode presumes that surrounding material exerts a *normal* restoring force on the deflecting fiber which is proportional to the deflection; i.e., a beam on a Winkler foundation. The first buckling load of a beam so restrained is a non-monotonic function of the beam length (or the wavelength of the buckling mode). The buckling load has a minimum value for some finite value of the wavelength. This optimum wavelength $2L_{\text{opt}}$ is given by

$$L_{\text{opt}} = \pi \left[\frac{EI}{E_T} \right]^{1/4} \quad (11)$$

where EI is the bending resistance of the fiber bundle, and E_T , the modulus of the foundation, has a value somewhere between the matrix modulus and the composite transverse modulus.

In evaluating this expression, one must be careful in assigning values to EI . Recall that this bundle is itself deforming in the shear mode. By the time the bundle reaches the state at which the fibers break, the shear restraint of the matrix within the bundle is extremely small. In fact, the fibers in the bundle are nearly decoupled from one another. If this is the case, then the EI should not be associated with perfect composite material which has the size and shape of the bundle. Rather, the fibers in the bundle each act as independent beams, which means that

$$EI = \frac{\pi}{2} NE_f a^4 \quad (12)$$

for a bundle of N fibers. One can then substitute this into (11) to obtain the following expression for the optimum wavelength

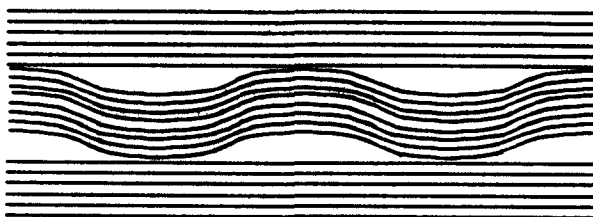


Fig. 9. Schematic of normal constraint provided by surrounding aligned material.

$$L_{\text{opt}} = \pi a \left[\frac{\pi}{2} N \frac{E_f}{E_T} \right]^{1/4} \quad (13)$$

For a relatively wide range in the choices of parameters N , E_f and E_T , one finds that the optimum wavelength is on the order of 10 to 20 times the fiber radius. In fact, Hahn and Sohi showed that the lengths of the kinked segments of their fiber bundles do, in fact, increase approximately linearly with $(E_f/E_T)^{1/4}$.

It must be noted that a linear relation between a wavelength and $(E_f/E_T)^{1/4}$ has been found by others (see, for example, Lanir and Fung, 1972). In fact, any analysis of elastic micro-buckling with normal matrix constraint—as in the extension mode—would predict this result. However, those analyses predict micro-buckling strains that are far above the observed values. We are suggesting here that the role played by the normal constraint is simply to determine the feasible range of imperfection wavelengths. Once the possible range of wavelength is established, then the shear mode analysis of the present theory, with the limited matrix shear response, the finite deflections of the fiber, and the breaking of the fibers at the points of maximum tensile strain, should apply.

Though the fiber breaking strain appeared to be insensitive to the matrix modulus (considering α'), some experiments indicate that it does affect the compressive strength. The following explanation for this dependence is suggested. Lower values of matrix modulus lead to wider kinks. Even though the kink width depends weakly on E_m ($L/a \sim (E_f/E_m)^{1/4}$, assuming E_T scales with E_m), the fiber breaking strain is very sensitive to the kink width. This explanation could be tested by carefully noting the kink widths for a set of composites with progressively stiffer matrices.

CONCLUSIONS

A theory has been proposed for calculating the initiation of fiber breaks that accompany kinking. It is based on an initially misaligned fiber bundle that is capable of *finite* deflections, and on elastic-plastic shear resistance of the matrix. The criterion for fiber breakage is that the maximum tensile strain in the fibers is equal to the fiber failure strain. The theoretical fiber breaking strains depend most sensitively on the kink width; remarkably, though, they are found to correspond reasonably well with observed compressive failure strains when the kinks are assumed to have the observed widths. It is suggested that the transverse constraint of material surrounding the misaligned bundle plays a role in determining the kink width and, thereby, the fiber failure strain. The reasonable agreement between the fiber breaking strain and the compressive strength suggests that the breaking of the fibers is the limiting step in forming the kink. Further exploration of this point is found in Part II in which the actual formation of the kink band is studied.

Acknowledgements—The author appreciates a discussion with L. G. Papanizos which prompted the initial post-buckling analysis. Support by the Department of Mechanical Engineering, Carnegie Mellon University is gratefully acknowledged.

REFERENCES

- Argon, A. S. (1972). Fracture of composites. In *Treatise on Materials Science and Technology* 1, 79–114. Academic Press, New York.
- Berg, C. A. and Salama, M. (1973). Fatigue of graphite fiber-reinforced epoxy in compression. *Fibre Sci. Tech.* 6, 79–118.
- Budiansky, B. (1974). Theory of buckling and post-buckling behavior of elastic structures. In *Advances in Applied Mechanics* 14, 1–63. Academic Press, New York.
- Budiansky, B. (1983). Micromechanics. *Computers and Structures* 16, 3–12.
- Chaplin, C. R. (1977). Compressive fracture in unidirectional glass-reinforced plastics. *J. Mat. Sci.* 12, 347–352.
- Chung, W.-Y. and Testa, R. B. (1969). The elastic stability of fibers in a composite plate. *J. Comp. Mat.* 3, 58–80.
- Dow, N. F. and Grunfest, I. J. (1960). Determination of most needed potentially possible improvements in materials for ballistic and space vehicles. GE-TIS 60SD389.
- Evans, A. G. and Adler, W. F. (1978). Kinking as a mode of structural degradation in carbon fiber composites. *Acta. Met.* 26, 725–738.

- Greszczuk, L. B. (1975). Microbuckling failure of circular fiber-reinforced composites. *AIAA* 13, 1311–1318.
- Greszczuk, L. B. (1982). On failure modes of unidirectional composites under compressive loading. In *Fracture of Composite Materials* (Edited by G. C. Sih and V. P. Tamuzs), pp. 231–244. Martinus Nijhoff Publishers, The Hague.
- Hahn, H. T. (1987). Compressive failure of unidirectional composites. *13th Annual Int. Symp. for Testing and Failure Analysis*. Los Angeles, California.
- Hahn, H. T. and Sohi, M. M. (1986). Buckling of a fiber bundle embedded in epoxy. *Comp. Sci. Tech.* 27, 25–41.
- Herrmann, L. R., Mason, W. E. and Chan, S. T. K. (1967). Response of reinforcing wires to compressive states of stress. *J. Comp. Mat.* 1, 212–226.
- Lanir, Y. and Fung, Y. C. B. (1972). Fiber composite columns under compression. *J. Comp. Mat.* 6, 387–401.
- Piggott, M. R. (1981). A theoretical framework for the compressive properties of aligned fibre composites. *J. Mat. Sci.* 16, 2837–2845.
- Piggott, M. R. and Harris, B. (1980). Compression strength of carbon, glass and Kevlar-49 fibre reinforced polyester resins. *J. Mat. Sci.* 15, 2523–2538.
- Rosen, B. W. (1965). Mechanics of composite strengthening. *Fiber Composite Materials*, pp. 37–75. American Society for Metals, Metals Park, Ohio.
- Sadowsky, M. A., Pu, S. L. and Hussain, M. A. (1967). Buckling of microfibers. *J. Appl. Mech.* 34, 1011–1016.
- Steif, P. S. (1987). An exact two-dimensional approach to fiber micro-buckling. *Int. J. Solids Structures* 23, 1235–1246.
- Steif, P. S. (1988). A simple model for the compressive failure of weakly bonded, fiber-reinforced composites. *J. Comp. Mat.* 22, 818–828.
- Weaver, C. W. and Williams, J. G. (1975). Deformation of a carbon-epoxy composite under hydrostatic pressure. *J. Mat. Sci.* 10, 1323–1333.
- Waas, A. M., Babcock, C. D. and Knauss, W. G. (1990). Mechanical model for elastic fiber micro-buckling. *J. Appl. Mech.* (to be published).

APPENDIX

In this Appendix the solution to the linearized equation with elastic–perfectly plastic matrix response is outlined. Again, it is assumed that there is a sinusoidal imperfection. If the load k is less than $T_f(1+\alpha)/(T_f+e)$, then the matrix responds elastically all along its length, and the solution is

$$\theta = \frac{\alpha+1}{\alpha+1-k} e \cos x. \quad (\text{A1})$$

Once k exceeds this value the matrix responds plastically along $0 < x < x_f$ and elastically along $x_f < x < \pi/2$. At the point x_f , the shear strain θ is precisely equal to the value needed to initiate plasticity; that is,

$$\theta(x_f) = \theta_0(x_f) + T_f. \quad (\text{A2})$$

The solution is given by

$$\theta = \frac{\cos \sqrt{k}x}{\cos \sqrt{k}x_f} \left\{ T_f \left[1 - \frac{\alpha}{k} \right] - \frac{ek}{1-k} \cos x_f \right\} + \frac{e}{1-k} \cos x + \frac{\alpha T_f}{k} \quad (0 < x < x_f) \quad (\text{A3a})$$

$$\theta = \frac{\sinh \lambda x - \tanh \frac{\lambda \pi}{2} \cos \lambda x}{\sinh \lambda x_f - \tanh \frac{\lambda \pi}{2} \cos \lambda x_f} \left[T_f - \frac{ek}{\alpha+1-k} \cos x_f \right] + \frac{\alpha+1}{\alpha+1-k} e \cos x \quad \left(x_f < x < \frac{\pi}{2} \right) \quad (\text{A3b})$$

when $\lambda = \sqrt{\alpha-k}$.

Finally, one must impose the condition that the moment is continuous at $x = x_f$. This implies that the derivative $\theta'(x_f)$ is continuous, from which x_f may be determined.